JOURNAL OF GEOPHYSICAL RESEARCH, VOL. 105, NO. B9, PAGES 21,497–21,508, SEPTEMBER 10, 2000

Impact of atmospheric water vapor on the thermal infrared remote sensing of volcanic sulfur dioxide emissions: A case study from the Pu'u 'O'o vent of Kilauea Volcano, Hawaii

Vincent J. Realmuto and Helen M. Worden

Jet Propulsion Laboratory, Pasadena, California

Abstract. The December 18, 1999, launch of NASA's Terra satellite put two multispectral thermal infrared imaging instruments into Earth orbit. Experiments with airborne instruments have demonstrated that the data from such instruments can be used to detect volcanic SO_2 plumes and clouds. However, one of the greatest challenges that will confront efforts to monitor volcanic SO_2 emissions from space is the need to characterize the local atmosphere. In this paper we evaluate the sensitivity of the SO_2 retrieval procedure to our knowledge of the local atmospheric conditions. We compare SO_2 retrievals obtained with distant (radiosonde) and local (Fourier transform infrared (FTIR) soundings) atmospheric measurements and find that the relative difference is typically $\pm 25\%$. For ground temperature retrievals the relative difference is $\pm 1.5\%$. These results lead us to conclude that while local measurements of atmospheric conditions are preferable, useful retrievals can be obtained using atmospheric measurements from distant sites. In addition, we find very good agreement between SO_2 and ground temperature retrievals obtained from thermal infrared imagery and FTIR soundings.

1. Introduction

Measurements of the rates of sulfur dioxide (SO_2) emission from volcanoes have been used to infer magma supply rates [e.g., *Casadevall et al*., 1981, 1983; *Chartier et al*., 1988; *Williams et al*., 1990; *Andres et al*., 1991], to estimate the contributions of volcanoes to the global SO_2 budget [e.g., *Stoiber et al*., 1987; *Berresheim and Jaeschke*, 1993; *Kyle et al*., 1994; *Graf et al*., 1997], and to determine the emission rates of other constituents of volcanic plumes [e.g., *Rose et al*., 1986, 1988; *Kyle et al*., 1990; *Zreda-Gostynska and Kyle*, 1993]. Long-term SO_2 monitoring programs provide the time series data sets necessary to establish baseline emission rates, to document departures from baseline emission, and to correlate changes in emission rates with volcanic phenomena [e.g., *Casadevall et al*., 1983, 1987; *Chartier et al*., 1988; *McGee*, 1992; *Elias et al*., 1993; *Caltabiano et al*., 1994; *Kyle et al*., 1994; *Zapata et al*., 1997]. For example, the routine monitoring of Mount Etna emissions since 1987 has led *Bruno et al*. [1999] to suggest that the style of eruptive activity can be predicted from the rate at which Etna's SO_2 emissions increase prior to an eruption. In other examples, *McGee and Sutton* [1994] reported that exogenous dome-building events at Mount St. Helens were typically preceded by increases in gas emissions, and *Daag et al*. [1996] correlated fluctuations in SO_2 emission rates preceding the 1991 eruptions of Mount Pinatubo to the rise of fresh magma, followed by the partial sealing of the magma system, emergence and growth of the lava dome, and reopening of the magma system prior to the initial Plinian eruption.

Realmuto et al. [1994, 1997] and *Teggi et al*. [1999] have demonstrated the use of airborne multispectral thermal infrared (TIR) remote sensing to map volcanic SO_2 plumes. These studies illustrated the potential of TIR remote sensing for monitoring volcanic SO_2 emissions, but the airborne mode of data collection is too expensive and labor intensive for routine monitoring programs. With the December 18, 1999, launch of Terra, a NASA Earth Observing System (EOS) satellite, the collection of multispectral TIR image data over much of the surface of the Earth will become more commonplace. These data will be acquired by the Advanced Spaceborne Emission and Reflection Radiometer (ASTER) [*Kahle et al*., 1991; *Yamaguchi et al*., 1998] and the Moderate Resolution Imaging Spectroradiometer (MODIS) [*Barnes et al*., 1998]. Recent model simulations [*Realmuto*, 2000] suggest that both ASTER and MODIS will have sufficient spatial and signal resolution to detect Mount Etna-scale SO_2 plumes and that ASTER will be able to resolve Kilauea (Pu'u 'O'o)-scale plumes.

The estimation, or retrieval, of SO_2 concentrations from radiance measurements requires the use of models that calculate the absorption of ground radiance en route to a sensor together with the radiance emitted by the atmosphere. Such radiative transfer models require the input of altitude profiles of atmospheric pressure, temperature, relative humidity, and composition. Given the difficulty in measuring such profiles directly, characterization of the local atmosphere represents a major challenge to the routine monitoring of volcanic SO_2 emissions from space.

The standard technique for characterizing the atmosphere is to launch balloon-borne sondes that transmit measurements of atmospheric pressure, temperature, and relative humidity to ground receiving stations. This procedure requires dedicated field personnel and radiosonde equipment that may be prohibitively expensive. Government weather agencies, such as the U.S. National Weather Service (NWS), may maintain networks of radiosonde launch sites, but a launch site can be distant from the field of interest or the launches too infrequent to coincide with a satellite overpass. In addition, some varieties of radiosondes have demonstrated systematic errors in the mea-

Paper number 2000JB900172.
0148-0227/00/2000JB900172$09.00

surement of water vapor (cf. *Wade* [1994] or *Ferrare et al*. [1995]).

In practice, the most difficult parameters to characterize are the spatial and temporal distributions of atmospheric water vapor. Maps of the column abundance of water vapor derived from airborne imaging spectrometer data indicate spatial variations on the scale of 20 m [*Carrere and Conel*, 1993]. Spatial variations such as these cannot be characterized by a radiosonde launched from a single location. Multiple radiosonde launches would also be required to characterize temporal variations, since a sonde typically spends a fraction of a second at any given altitude. Tethered sonde systems can provide time series data at a limited number of altitudes, but such systems are more expensive and complicated than free-flying radiosondes.

Given the difficulty of characterizing the local atmosphere, satellite-based monitoring of volcanic SO_2 emissions will not become routine if the SO_2 retrievals are overly sensitive to the local atmospheric conditions. In this paper we describe an experiment designed to evaluate the sensitivity of SO_2 and ground temperature retrievals derived from thermal infrared multispectral scanner (TIMS) data to knowledge of the local atmospheric conditions. We will compare the retrievals obtained with a distant radiosonde measurement with those obtained with coincident atmospheric measurements acquired by the Airborne Emission Spectrometer (AES). In addition, we will compare independent retrievals derived from TIMS and AES data in an effort to validate the respective retrieval procedures.

2. Data Collection and Processing

On December 9, 1996, AES and TIMS data were acquired over an SO_2 plume emitted from the Pu'u 'O'o vent of Kilauea Volcano, Hawaii (Plate 1). The instruments were flown in NASA's DC-8 research aircraft at an altitude of 8.6 km (mean sea level, MSL). The 1996 DC-8 deployment marked the first simultaneous use of TIMS and AES in a flight experiment.

AES (Figure 1) is an open-path Fourier transform infrared (OP-FTIR) spectrometer [cf. *Beer*, 1992] that can acquire radiance measurements in over 32,000 spectral channels between 3.3 and 14.3 μm [*Worden et al*., 1997], although our analysis is limited to data collected between 7.4–9.5 and 11.1–13.3 μm. While the use of ground-based OP-FTIR spectrometers to estimate the SO_2 concentration of volcanic plumes is well established [*Naughton et al*., 1969; *Mori et al*., 1993; *Francis et al*., 1995; *Love et al*., 1998], we believe that our flight experiment is the first application of a downward looking airborne OP-FTIR spectrometer to such an investigation.

The use of TIMS data to map volcanic SO_2 plumes has been discussed by *Realmuto et al*. [1994, 1997] and *Realmuto* [2000], and the principles of SO_2 retrieval in the thermal infrared are the same for either TIMS or AES data. The presence of SO_2 in a plume results in the absorption and emission of radiance between 8 and 9.5 μm (Figure 2). The strengths of the absorption and emission are a function of both SO_2 concentration and the temperature contrast between the plume and ground, with temperature contrast as the dominant factor [*Realmuto*, 2000]. Since we must know the temperature of the plume, we restrict our retrievals to the passive, or nonbuoyant, portion of a plume, which is in thermal equilibrium with the surrounding atmosphere. The passive portion of a plume is generally cooler than the ground beneath it and the entrained SO_2 absorbs ground radiance in transit to the sensor. We employ radiative transfer modeling to find the concentration of SO_2 necessary to produce the observed attenuation of ground radiance.

MAP_SO2 is the procedure developed to estimate SO_2 concentrations from TIR image data. Although TIMS data were used in the development of MAP_SO2, the procedure is not limited to data from this sensor. MAP_SO2 is based on the MODTRAN radiative transfer code [*Berk et al*., 1989], which contains spectral band models for SO_2 and 11 other atmospheric gases. The band models have three temperature-dependent parameters (absorption coefficient, line density, and average line width) and are valid for gas temperatures between 200 and 300 K. In the version of MODTRAN used in our study the band models are based on the 1986 edition of the HITRAN spectral line atlas [*Rothman et al*., 1987]. The input to MAP_SO2 includes the observed radiance spectra, atmospheric pressure, temperature and relative humidity profiles, plume altitude and thickness, and elevation and emissivity of the background. MAP_SO2 produces maps of SO_2 column abundance (the product of SO_2 concentration and plume thickness) estimates, ground temperature estimates, and least squares misfits between the observed and model radiance spectra.

The high spectral resolution of the AES data permitted the simultaneous retrieval of atmospheric water vapor profiles, SO_2 concentration estimates, and ground emissivity and temperature estimates. These retrievals are based on the sequential evaluation algorithm for simultaneous and concurrent retrieval of atmospheric parameter estimates, or SEASCRAPE [*Sparks*, 1995, 1997], radiative transfer code. SEASCRAPE employs the 1996 edition of the HITRAN line atlas [*Rothman et al*., 1998], together with additional water vapor continuum [*Clough et al*., 1989] and line [*Toth*, 1998; *Toth et al*., 1998] parameters, to calculate radiance spectra.

The input to SEASCRAPE includes a priori estimates of the model parameters, together with uncertainties that characterize our prior knowledge of these parameters. SEASCRAPE produces a final set of estimates that minimizes the weighted least squares misfit between the observed and calculated radiance spectra. In addition to a priori estimates of model parameters we specified constraints on the range of acceptable values for selected model parameters. SEASCRAPE is a line by line radiative transfer code, calculating radiance spectra based on individual spectral lines rather than band models, and is not restricted to a range of gas temperatures.

AES was operated in a step and stare mode due to the variations in background emissivity (cf. Plate 2a). In this mode AES is aimed at selected ground targets through the use of a pointing mirror (Figure 1) and a series of interferograms, which we will refer to as scans, are collected. Four ground targets were selected along the flight path: a site in the forest canopy upwind of Pu'u 'O'o (cf. Plate 1), a site near the vent, a site downwind of Pu'u 'O'o near Holei Pali (pali is the Hawaiian word for a cliff or steep break in slope), and a site over the Pacific Ocean.

Given our assumption that the Pu'u 'O'o plume was in thermal equilibrium with the surrounding atmosphere, the temperature of the plume was defined by its altitude and thickness. We could not make independent measurements of plume altitude or thickness during the 1996 DC-8 overflight, so we obtained these dimensions from a cross-section of a Pu'u 'O'o plume determined by an airborne survey on September 19, 1995 [*McGee and Gerlach*, 1998]. Our use of the 1995 plume dimensions is justified by the similarity in wind conditions

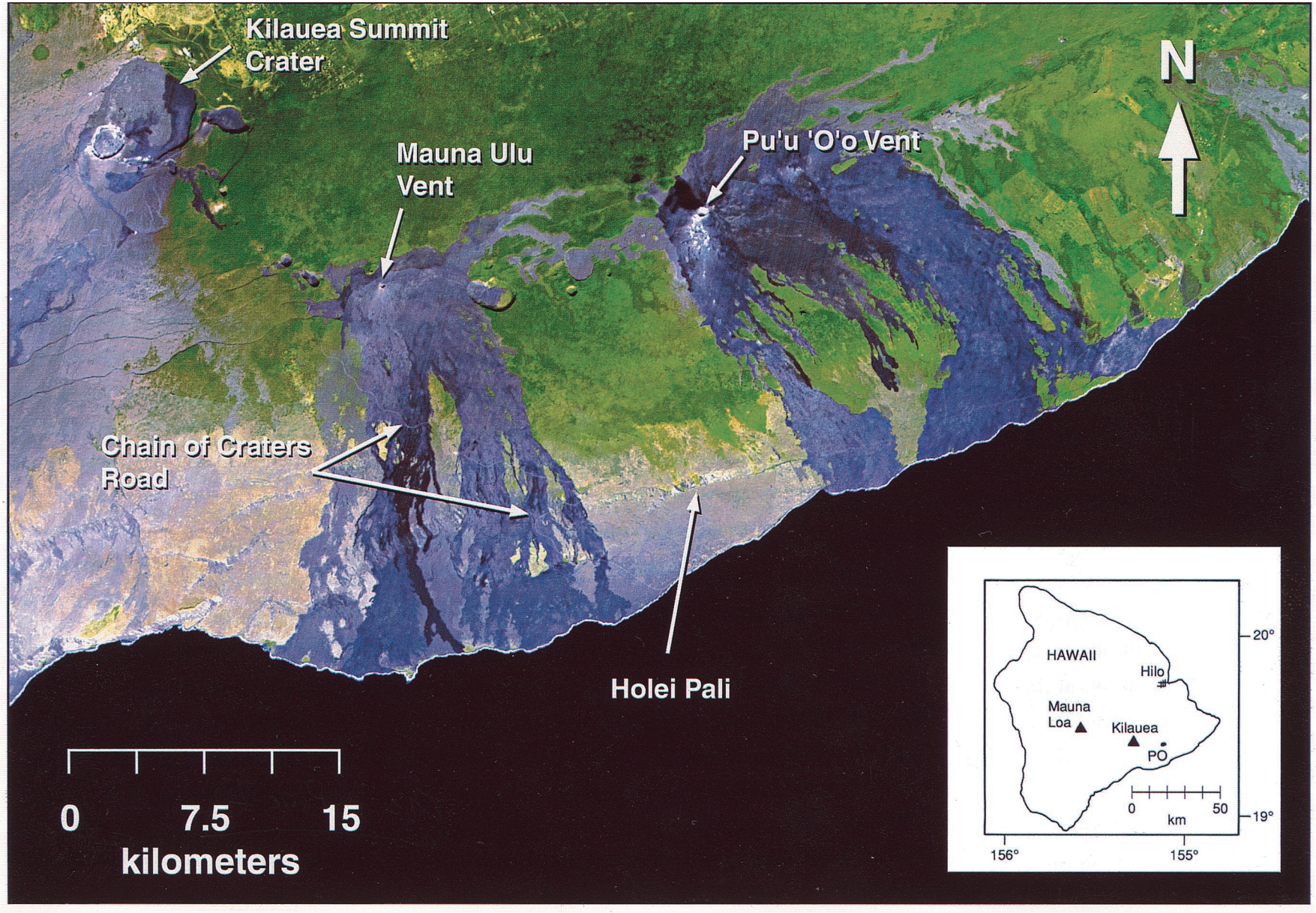

Plate 1. Annotated satellite image of the southeastern flank of Kilauea Volcano, Hawaii. The image shows the locations of the summit crater of Kilauea, the Pu'u 'O'o and Mauna Ulu vents, and Holei Pali. The inset map shows the location of the summit of Kilauea and the Pu'u 'O'o (PO) vent relative to Hilo, the launch site for National Weather Service radiosondes.

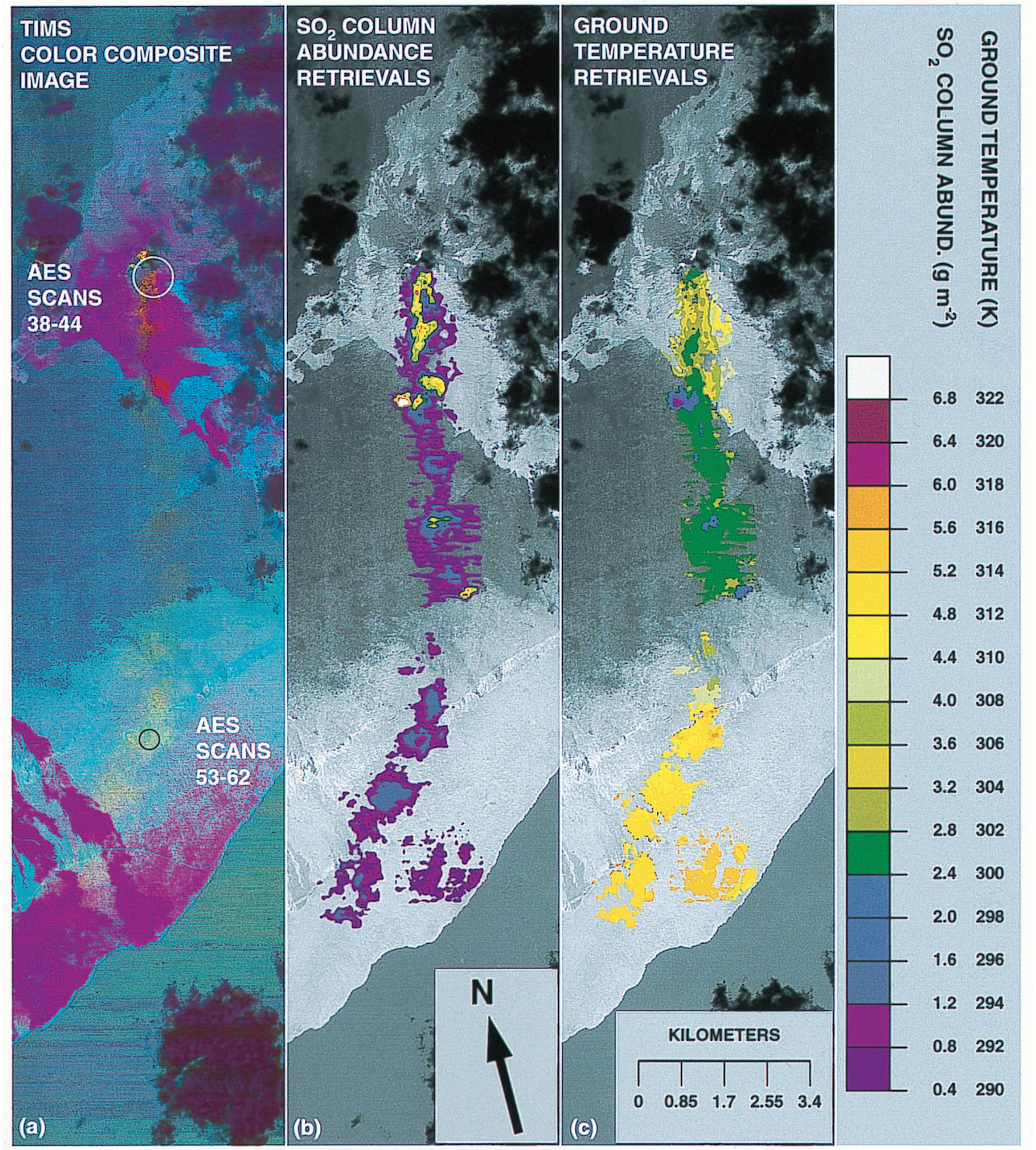

Plate 2. Mosaic of TIMS data and output of the MAP_SO2 retrieval procedure. (a) False color composite of TIMS data, showing approximate locations of the AES target sites at Pu'u 'O'o and Holei Pali. The circles represent our uncertainty regarding the pointing accuracy of AES. (b) Color contour map of the MAP_SO2 SO_2 column abundance retrievals. (c) Color contour map of the MAP_SO2 ground temperature retrievals. The contour intervals are indicated in the attached color bar.

during the 1995 and 1996 surveys. During the 1995 survey the winds in the vicinity of Pu'u 'O'o were blowing from the northeast at a speed of 5.65 m s^{-1} [*McGee and Gerlach*, 1998], while during the 1996 survey the winds were blowing from the north at a speed of 8.5 m s^{-1} (J. Sutton, personal communication, 2000). Furthermore, since our objective was to compare the retrievals from MAP_SO2 and SEASCRAPE, the use of the same plume dimensions in each procedure was more important than the absolute accuracy of the dimensions.

The 1995 cross section [*McGee and Gerlach*, 1998] showed that the plume was ~1 km thick, with a center line, or midpoint, altitude of ~1.25 km (MSL). MODTRAN and SEASCRAPE

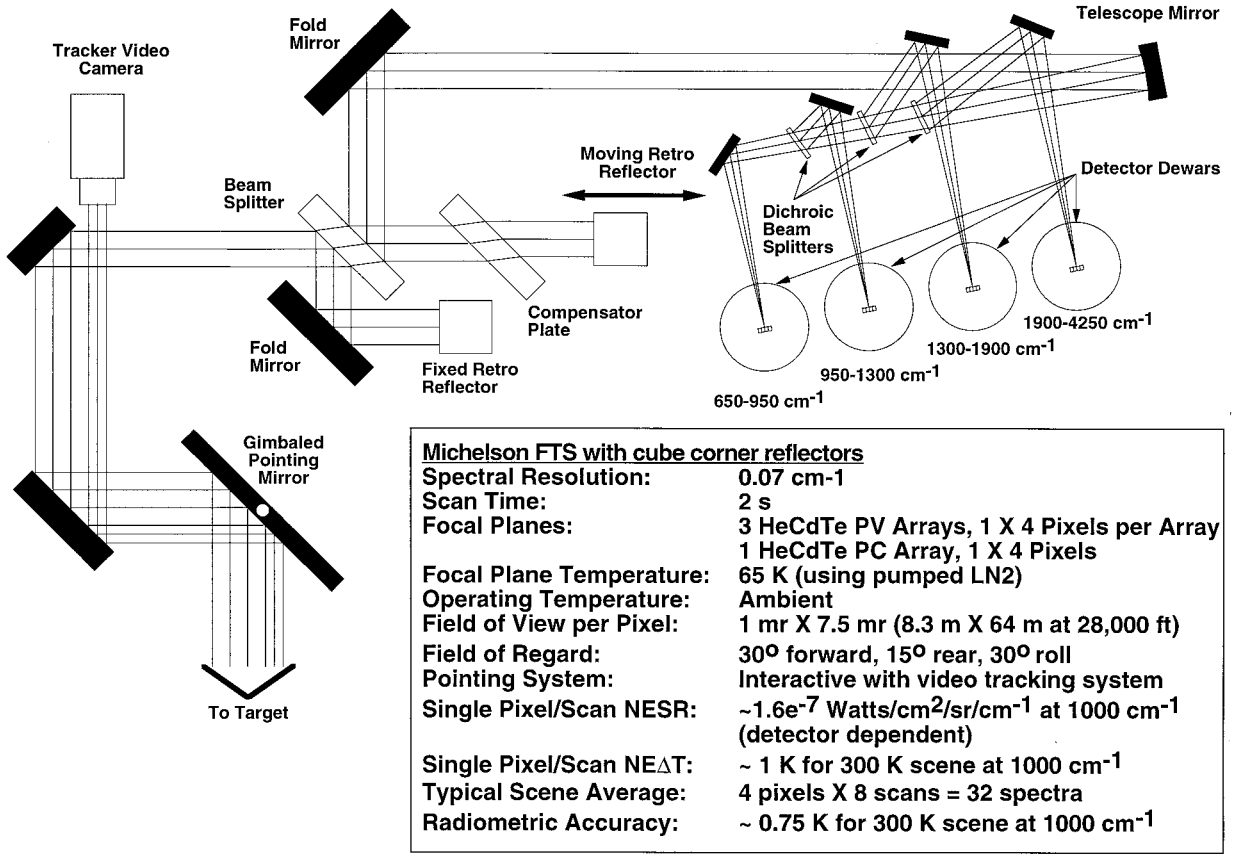

Figure 1. Optical layout and specifications of the airborne emission spectrometer (AES).

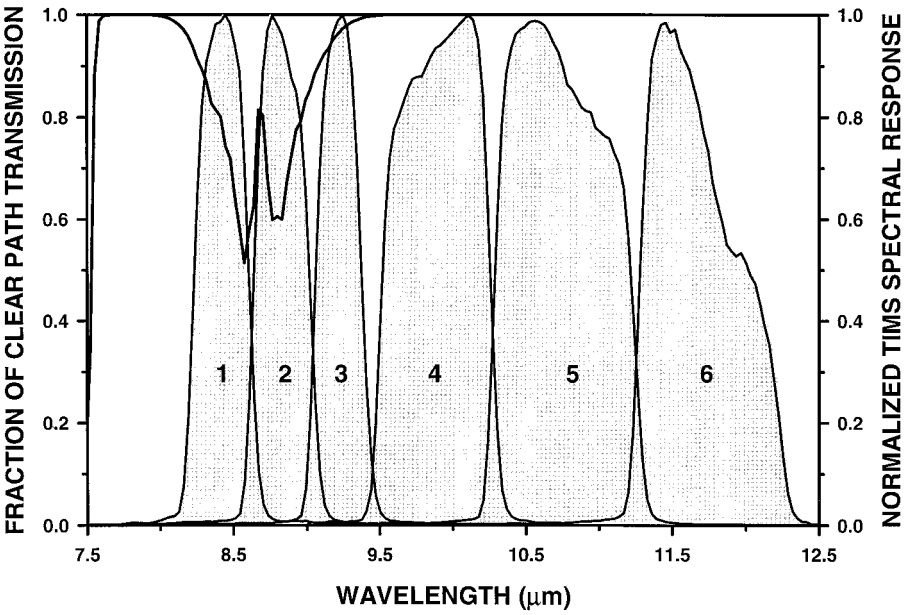

Figure 2. Comparison of the transmission spectra of two atmospheric columns, as calculated with MODTRAN. The inputs to MODTRAN included the ocean atmosphere profile derived from the AES data (Figure 3), ground and sensor altitudes of 0.001 and 8.6 km, respectively, and a ground temperature of 305 K. The plot depicts the ratio of the transmission through a column containing 10 g m^{-2} SO_2 to that of a column containing no SO_2 (i.e., clear path transmission). The shaded regions represent the normalized spectral response functions of the six TIMS channels (as of May 1, 1996).

operate on a layered, or plane-parallel, model of the atmosphere, and we assigned one layer of the model atmosphere to the SO_2 plume. One consequence of this approach is that the midpoint altitude of the plume must be at least one plume thickness (i.e., 1 km) above the ground elevation. Therefore, wherever the ground elevation exceeded 0.25 km, the midpoint altitude input to MODTRAN and SEASCRAPE exceeded 1.25 km.

The atmospheric pressure, temperature, and humidity profiles employed in our study were measured by a NWS radiosonde launched from the Hilo Airport, which is located ~37.5 km north of Pu'u 'O'o (Plate 1). Although the launch site was distant from experiment site, the time of the launch (2304 UT, 1304 HST) coincided with the DC-8 overflight of Pu'u 'O'o (2322 to 2325 UT).

3. Discussion

3.1. MAP_SO2 Output

Plate 2a depicts a color composite of the imagery acquired in TIMS channels 5, 3, and 2 (Figure 2) displayed in red, green and blue, respectively. The spectral contrast of these data were enhanced with the decorrelation stretch algorithm [*Gillespie et al*., 1986] prior to compositing, and Plate 2a represents variations in emissivity and temperature as variations in display color and brightness, respectively. The absorption of ground radiance in TIMS channel 2 by the SO_2 plume (Figure 2) is represented by a reduction in the blue component of the color composite image, and the plume is rendered in hues of yellow and red (Plate 2a). Lava tubes adjacent to Pu'u 'O'o are delineated by the alignment of bright yellow patches, which represent the SO_2 emissions from holes, or skylights, in the roofs of the lava tubes. The chromatic variations observed within the Pu'u 'O'o flow field are primarily due to variations in age, surface texture, and exposure to acidic aerosols, as described by *Realmuto et al*. [1992], *Crisp et al*. [1990], and *Kahle et al*. [1988].

Plate 2a also shows the approximate locations of the AES target sites near Pu'u 'O'o and Holei Pali (compare Plate 1). The AES spectra from the Pu'u 'O'o and Pali sites represent the averages of six (scans 38–44) and nine (scans 53–62) scans, respectively. The circles (Plate 2a) represent our uncertainty as to the exact location of the AES footprints. This uncertainty is the summation of inaccuracies in the pointing of AES and our knowledge of the roll, pitch, and yaw of the aircraft. The ground resolution of the AES and TIMS radiance measurements was approximately 34 by 64 m and 8.5 m, respectively.

Plates 2b and 2c are color-contoured versions of the SO_2 column abundance and ground temperature estimates, respectively, produced with MAP_SO2. The SO_2 abundance generally ranged between 0.4 and 2.4 g m^{-2}, with the exception of several high-concentration (4–7.5 g m^{-2}) cells, or puffs, near Pu'u 'O'o. The apparent bifurcation of the puff closest to Pu'u 'O'o (Plate 2b) represents the contribution of SO_2 vented from skylights to the main plume. As an aside, we note that the near-vent portion of the plume had sufficient opacity to shade, and thereby cool, the ground beneath it (Plate 2c).

At least two of the puffs that appear over the forested region between the Pu'u 'O'o flow field and Holei Pali (compare Plate 1) can be attributed to meteorological clouds [cf. *Realmuto et al*., 1997; *Realmuto*, 2000]. These spurious puffs are identified through their association with anomalously low ground temperature estimates, which are 5–7 K cooler than the surrounding temperatures (Plate 2c). The meteorological clouds also appear dark, or cold, in the color composite image (Plate 2a). We did not specify any meteorological cloud parameters to MODTRAN, and therefore any attenuation of ground radiance by these clouds was attributed to SO_2 absorption and low ground temperatures.

The plume turned inland (to the west) over the coastal region between Holei Pali and the Pacific Ocean (Plate 2b). This turn was probably caused by on-shore winds blowing off the ocean. The interaction of the prevailing and on-shore winds appears to have created a small (1.7 km in diameter) eddy that trapped a quantity of SO_2.

3.2. Water Vapor Profiles

TIMS and AES observed the ground along the same optical path through the atmosphere at virtually the same time. In addition, AES collected spectra at multiple locations along the TIMS flight line. Therefore the water vapor profiles generated from the AES data provided better spatial and temporal resolution than the Hilo radiosonde profile. In this section we will evaluate the effects of this improvement on the output of MAP_SO2. We did not modify the Hilo temperature profile prior to the use of these data in either MAP_SO2 or SEASCRAPE.

A comparison of the water vapor profile measured at Hilo with those derived from AES data over three ground targets (Figure 3) reveals that the Hilo profile was generally more humid than any of the AES profiles. This result is consistent with the fact that Hilo normally receives more precipitation than the southeastern flank of Kilauea Volcano (315–380 versus 125–250 cm yr^{-1} [*Armstrong*, 1973]). In addition, carbon hygrister-style radiosondes, such as the one launched from Hilo, have documented calibration errors when relative humidity falls below 20% [*Wade*, 1994]. Comparisons of water vapor profiles measured with a variety of methods, including carbon hygrister sondes, demonstrate that carbon hygristers overestimate relative humidity when the ambient humidity is low [*Ferrare et al*., 1995].

This bias was evident in a comparison of humidity measurements made by a dew point hygrometer aboard the NASA DC-8 and the Hilo radiosonde. At flight altitude (8.6 km) the hygrometer measured a relative humidity of 6% (71 ppmv H_2O), whereas the sonde measured a relative humidity of 25% (275 ppmv H_2O). In contrast, the AES profiles agreed with the DC-8 hygrometer measurement at 8.6 km (Figure 3).

Given that the Hilo water vapor profile was suspect, these data were modified before their use in MAP_SO2. We reduced the total column amount of water vapor in the profile as indicated by inspections of emissivity spectra calculated from TIMS radiance spectra collected over the ocean. The spectral emissivity of seawater at TIR wavelengths (8–14 μm) is known to be generally flat or featureless [*Salisbury and D'Aria*, 1992], so large variations in the calculated emissivity spectra can be attributed to atmospheric emission and absorption.

SEASCRAPE provided further evidence that the Hilo water vapor profile was not an accurate description of the atmosphere over Pu'u 'O'o. The initial use of these data as a priori estimates of water vapor resulted in unrealistic (i.e., negative) retrievals. To counter these results, we implemented nonnegative constraints in the retrieval process and then adjusted the a priori water vapor estimates until the nonnegative constraints were no longer necessary.

To evaluate the impact of the water vapor profiles on the MAP_SO2 retrievals, we computed a second set of SO_2 and

ground temperature retrievals using the AES profiles. We then calculated the difference between the retrievals obtained with the Hilo and AES profiles, relative to those obtained with the AES profiles. The choice of an AES profile (Figure 3) for an individual TIMS pixel was determined by ground elevation. For example, the Pali profile was not applied to pixels that represented ground elevations lower than the Pali target site (Plate 2a).

Figure 4a shows the distribution of the relative differences in SO_2 column abundance estimates as a histogram with a bin size of 10%. The mode of this distribution is centered on a relative difference of zero (±5%), and the majority of the differences (60%) fell between ±25%. The SO_2 column abundance estimates obtained with the AES profiles were generally larger than those obtained with the Hilo profile.

This sensitivity to water vapor is larger than that reported by *Realmuto et al*. [1994; 1997] for studies of TIMS data acquired over Mount Etna and Pu'u 'O'o, respectively. However, local measurements of atmospheric water vapor were not available in either of those studies. In the case of the Etna data (acquired on July 29, 1986) the sensitivity to water vapor was determined by modifying the total column amount of water vapor in a profile measured by a radiosonde launched from a site located 220 km from the volcano. In the case of the Pu'u 'O'o data (acquired on September 30, 1988), profiles measured by a NWS radiosonde launched from Hilo 4 hours after the TIMS data had been acquired were replaced with the MODTRAN tropical climatology model. In addition, the number of pixels involved in either sensitivity analysis was <100. In the current study we compared an entire SO_2 column abundance map derived with distant radiosonde profiles to a second map derived with local water vapor measurements, and this latest determination of sensitivity is probably the most accurate.

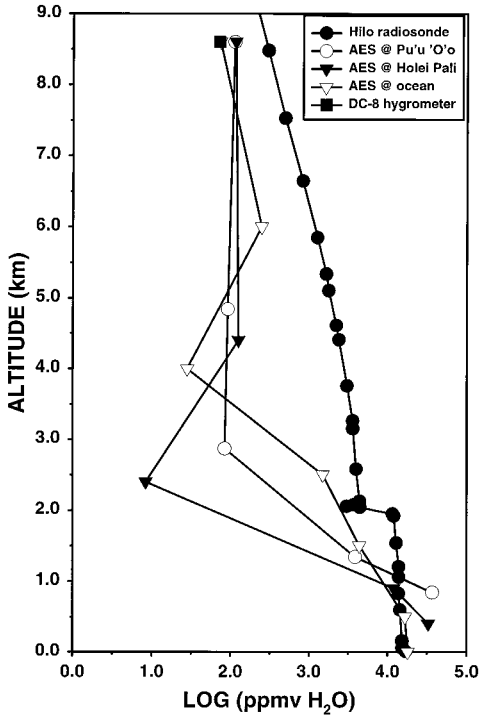

Figure 3. Comparison of the altitude profiles of atmospheric water vapor as measured by the Hilo radiosonde (solid circles) and derived from AES radiance measurements. Note that the AES-derived profiles converge on the humidity measurement from the DC-8 hygrometer (solid square) at the altitude of 8.6 km.

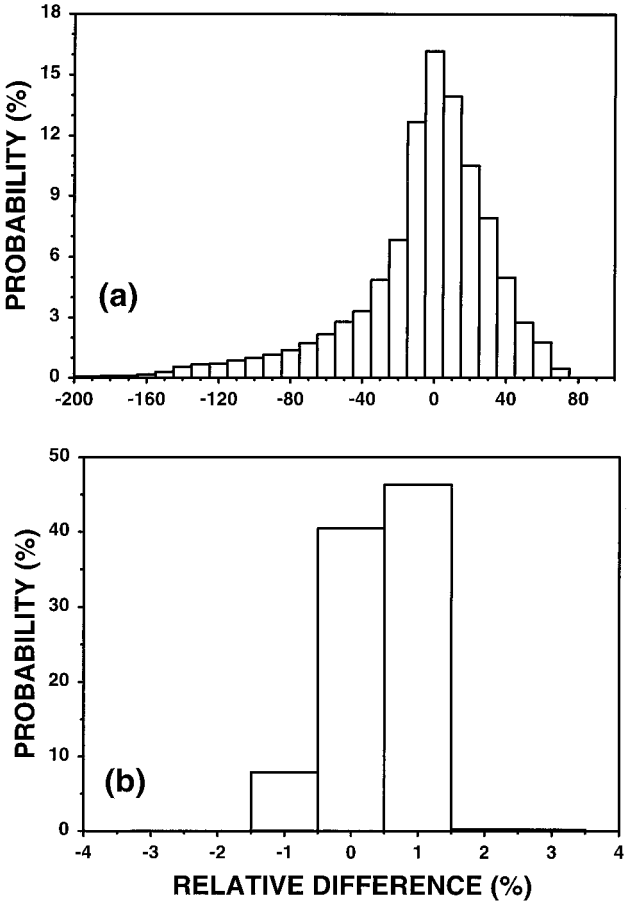

Figure 4. Histograms representing the distributions of the relative difference between MAP_SO2 retrievals derived with the Hilo water vapor profile and those derived with the AES profiles (Figure 3). (a) SO_2 column abundance. (b) Ground temperature.

The relative difference between the ground temperature estimates obtained with the Hilo and AES profiles was very small. As shown in Figure 4b, a histogram of the relative difference in temperature estimates, virtually all of the population had relative differences between ±1.5%. These results indicate that the TIMS-based retrieval algorithm returned different estimates of SO_2 column abundance in situations where the same ground temperature estimate was obtained with the Hilo and AES water vapor profiles; further demonstrating the dominant role of ground temperature in the observed radiance spectra.

3.3. Comparison of MAP_SO2 and SEASCRAPE Retrievals

In addition to the generation of water vapor profiles the AES radiance spectra collected at the Pu'u 'O'o and Pali target sites were used to estimate SO_2 concentration and ground temperature. We compared these estimates with those obtained from the TIMS radiance measurements over the same areas in an effort to validate the MAP_SO2 and SEASCRAPE retrieval procedures. To ensure against any bias, the MAP_SO2 retrievals used in the comparison were those derived with the Hilo water vapor profile (Plates 2b and 2c).

Table 1. Comparison of SEASCRAPE and MAP_SO2 Retrievals[a]

	SEASCRAPE		MAP_SO2	
Site	SO_2 Estimate, g m^{-2}	Ground Temperature Estimate, K	Mean SO_2 Estimate, g m^{-2}	Mean Ground Temperature Estimate, K
Pu'u 'O'o	4.86 ± 0.44	298.8 ± 1.0	4.81 ± 0.26	303.6 ± 1.6
Pali	0.70 ± 0.10	313.1 ± 1.0	0.75 ± 0.03	311.9 ± 0.9

[a]The spread in the SEASCRAPE retrievals represents systematic and random errors in the retrieval procedure; the spread in the MAP_SO2 results represents one standard deviation about the mean SO_2 column abundance and ground temperature estimate.

Plate 3 depicts the MAP_SO2 retrievals in the vicinity of the Pu'u 'O'o and Pali sites. To facilitate the comparison between the MAP_SO2 and SEASCRAPE retrievals, we resampled the SO_2 column abundance and ground temperature maps to the spatial resolution of the AES measurements (34 by 64 m). The results of our comparison are summarized in Table 1.

Our uncertainty as to the exact location of the AES footprints complicated the comparison of the MAP_SO2 and SEASCRAPE retrievals. We were required to search within the AES circles of uncertainty (Plate 3) for MAP_SO2 retrievals that matched either the SEASCRAPE SO_2 column abundance or ground temperature retrievals. Given the evidence that different water vapor profiles could lead to different SO_2 estimates with no corresponding change in the estimate of ground temperature (Figure 4), we decided to compare the ground temperature estimates that corresponded to equivalent MAP_SO2 and SEASCRAPE SO_2 column abundance estimates.

At the Pu'u 'O'o site (Plate 3a) we located the pixels that represented SO_2 column abundance estimates between 4.42 and 5.30 g m^{-2}. The mean of the MAP_SO2 ground temperature corresponding to this range of SO_2 estimates was 303.6 K, 4.8 K higher than the SEASCRAPE ground temperature estimate of 298.8 K. At the Pali site (Plate 3b) the mean of the MAP_SO2 ground temperature estimates corresponding to SO_2 estimates between 0.6 and 0.8 g m^{-2} was 311.9 K, 1.2 K lower than the SEASCRAPE ground temperature estimate of 313.1 K.

The comparisons suggest that the retrievals at the Pu'u 'O'o site were more sensitive to our knowledge of the local atmosphere than the Pali retrievals. However, physical differences between the sites may provide an alternate explanation for the results of the comparison. The Pu'u 'O'o site featured large variations in background temperature and emissivity, together with multiple SO_2 vents, within the AES circle of uncertainty. In addition, a portion of the circle appears to be outside of the plume (Plate 3a). In contrast, the Pali site featured a uniform temperature and emissivity background within the circle of uncertainty, and the entire circle was within a portion of the plume where the distribution of SO_2 was relatively uniform (Plate 3b). Thus the Pali site was more amenable to a comparison between the MAP_SO2 and SEASCRAPE retrievals.

4. Conclusions

The objectives of our research were to evaluate the sensitivity of TIR-based SO_2 retrievals to knowledge of the local atmospheric conditions and to validate the MAP_SO2 and SEASCRAPE retrieval procedures. The following conclusions are based on an experiment from a single volcano, and we urge caution before generalizing our results to other locations. However, the warm and humid tropical climate of Hawaii, coupled with the low altitude of the Pu'u 'O'o plume, conspire to create a worse-case scenario for the retrieval of SO_2 concentrations from TIR radiance measurements [cf. *Realmuto*, 2000]. Given the results of our experiment at Pu'u 'O'o, we are optimistic about the routine monitoring of SO_2 emissions from space with TIR remote sensing.

4.1. Sensitivity to Atmospheric Conditions

The difference between SO_2 column abundance estimates derived with water vapor profiles measured at a distant site (the Hilo profile) relative to estimates derived with coincident water vapor profiles (the AES profiles) was ±25%. This sensitivity to knowledge of atmospheric conditions is comparable to that of SO_2 estimates derived from correlation spectrometer (COSPEC) [*Moffat and Millan*, 1971; *Millan*, 1980; *Stoiber et al*., 1983] or total ozone mapping spectrometer (TOMS) [*Krueger et al*., 1995] data. Given that COSPEC and TOMS data have been applied to studies of a variety of volcanic plumes and clouds, under a variety of atmospheric conditions [e.g., *Andres et al*., 1993; *Bluth et al*., 1995, 1997; *Caltabiano et al*., 1994; *Krueger et al*., 1990; *Kyle et al*., 1990], the TIR-based retrieval of SO_2 should have a similar breadth of application.

4.2. Validation of Retrieval Procedures

The agreement between SO_2 column abundance and ground temperature estimates derived with MAP_SO2 and SEASCRAPE is a validation of these retrieval procedures. While the high spectral resolution of AES and sophistication of SEASCRAPE were necessary to retrieve water vapor profiles, our comparisons revealed that the low spectral resolution of TIMS and relative simplicity of MODTRAN were sufficient for the retrieval of SO_2 and ground temperature estimates.

4.3. Future Directions

Given the inherent difficulty of directly measuring atmospheric profiles, the use of profiles from model atmospheres is an attractive alternative. The MODTRAN software package contains profiles from five reference atmospheric models (subarctic summer, subarctic winter, midlatitude summer, midlatitude winter, and tropical), together with a U.S. Standard Atmosphere profile. However, the MODTRAN profiles offer little spatial or temporal resolution.

Global climate assimilation models generated with grid spacings of the order of 1° to 2° (of longitude and latitude) and time intervals of the order of 3 to 6 hours [*Kanamitsu*, 1989; *Schubert et al*., 1993] may provide the spatial and temporal resolution necessary to characterize local atmospheric condi-

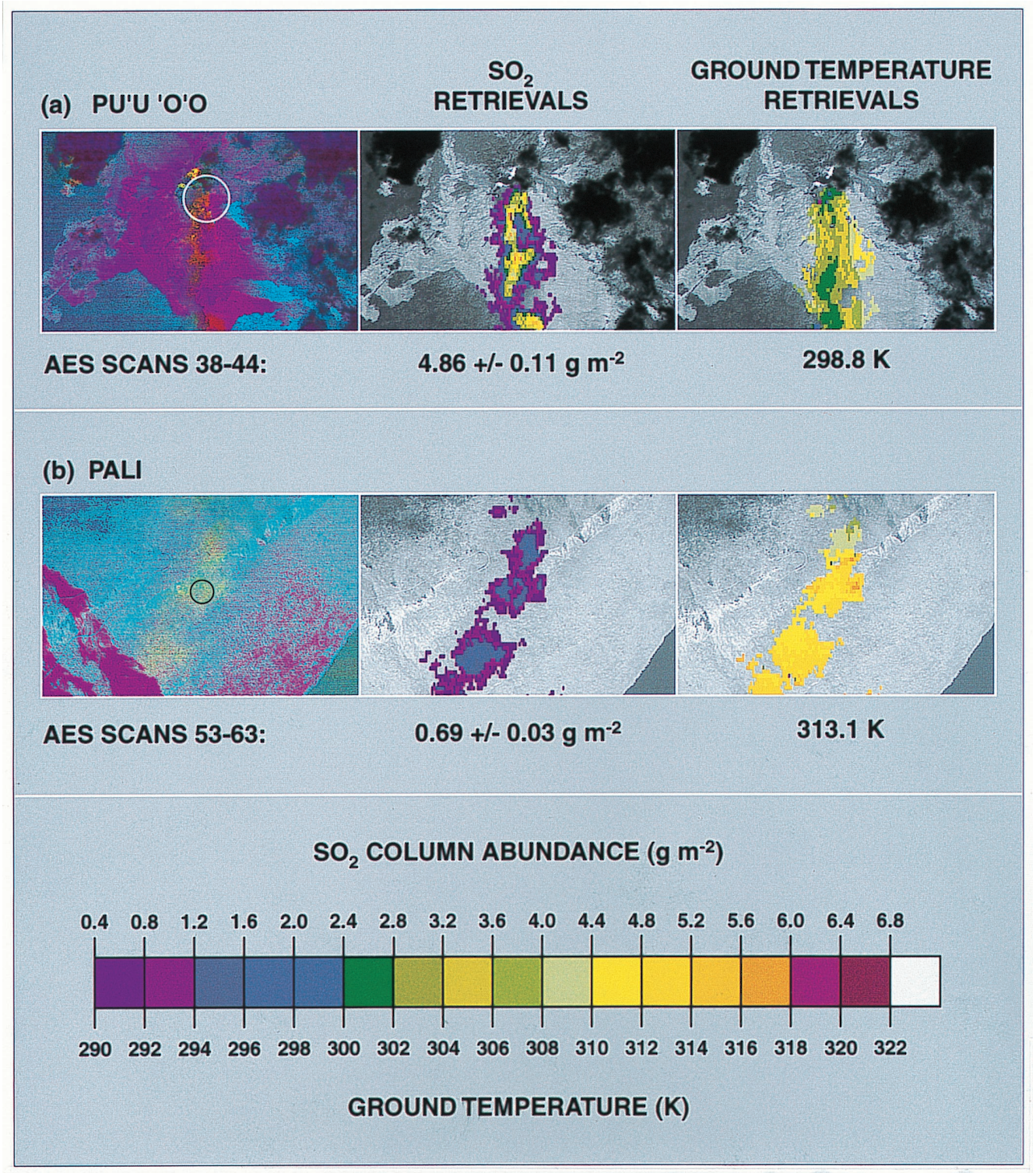

Plate 3. Comparison of the MAP_SO2 and SEASCRAPE retrievals. The spread in the SEASCRAPE results represents systematic and random errors in the retrieval procedure. The MAP_SO2 results have been resampled to the AES spatial resolution (34 × 64 m) to facilitate the comparison. (a) Pu'u 'O'o site. (b) Pali site.

tions. We are currently evaluating the use of profiles from such models in our retrieval procedures.

Acknowledgments. We recognize the efforts of our colleagues at the Airborne Science Program (NASA Dryden Flight Research Facility) and Airborne Sensor Facility (NASA Ames Research Center), without which we could not have collected the data for our experiment. We thank R. Beer and D. Rider of the Jet Propulsion Laboratory for their operation of AES during the Pu'u 'O'o overflights. J. Sutton and T. Elias of the USGS Hawaiian Volcano Observatory provided background information on Pu'u 'O'o as well as logistical support during the flight experiment. Our manuscript was greatly improved through careful reviews by W. Rose, S. Williams, and J. Eichelberger. This

research was conducted at the Jet Propulsion Laboratory, California Institute of Technology, under contract to the National Aeronautic and Space Administration.

References

Andres, R. J., W. I. Rose, P. R. Kyle, S. deSilva, P. Francis, M. Gardeweg, and H. Moreno-Roa, Excessive sulfur dioxide emissions from Chilean volcanoes, *J. Volcanol. Geotherm. Res*., *46*, 323–329, 1991.

Andres, R. J., W. I. Rose, R. E. Stiober, S. N. Williams, O. Matias, and R. Morales, A summary of sulfur dioxide emission rate measurements from Guatemalan volcanoes, *Bull. Volcanol*., *55*, 379–388, 1993.

Armstrong, R. W., *Atlas of Hawaii*, Univ. of Hawaii Press, Honolulu, 1973.

Barnes, W. L., T. S. Pagano, and V. V. Salomonson, Prelaunch characteristics of the moderate resolution imaging spectrometer (MODIS) on EOS-AM1, *IEEE Trans. Geosci. Remote Sens*., *36*, 1088–1100, 1998.

Beer, R., *Remote Sensing by Fourier Transform Spectrometry*, *Chem. Anal*., vol. 120, 153 pp., John Wiley, New York, 1992.

Berk, A., L. S. Bernstein, and D. C. Robertson, MODTRAN: A medium resolution model LOWTRAN-7, *Tech. Rep. GL-TR-89-0122*, Air Force Geophys. Lab., Hanscom AFB, Mass., 1989.

Berresheim, H., and W. Jaeschke, The contribution of volcanoes to the global atmospheric sulfur budget, *J. Geophys. Res*., *88*, 3732–3740, 1983.

Bluth, G. J. S., C. J. Scott, I. E. Sprod, C. C. Schnetzler, A. J. Krueger, and L. S. Walter, Explosive emissions of sulfur dioxide from the 1992 Crater Peak eruptions, Mount Spurr, Alaska, *U.S. Geol. Surv. Bull*., *2139*, 47–57, 1995.

Bluth, G. J. S., W. I. Rose, I. E. Sprod, and A. J. Krueger, Stratospheric loading of sulfur from explosive volcanic eruptions, *J. Geol*., *105*, 671–683, 1997.

Bruno, N., T. Caltabiano, and R. Romano, SO_2 emissions at Mt. Etna with particular reference to the period 1993–1995, *Bull. Volcanol.*, *60*, 405–411, 1999.

Caltabiano, T., R. Romano, and G. Budetta, SO_2 flux measurements at Mount Etna (Sicily), *J. Geophys. Res*., *99*, 12,809–12,819, 1994.

Carrere, V., and J. E. Conel, Recovery of atmospheric water vapor total column abundance from imaging spectrometer data around 940 nm—Sensitivity analysis and application to airborne visible/infrared imaging spectrometer (AVIRIS) data, *Remote Sens. Environ*., *44*, 179–204, 1993.

Casadevall, T. J., D. A. Johnston, D. M. Harris, W. I. Rose, L. L. Malinconico, R. E. Stoiber, T. J. Bornhorst, S. N. Williams, L. Woodruff, and J. M. Thompson, SO_2 emission rates at Mount St. Helens from March 29 through December 1980, in *The 1980 Eruptions of Mount St. Helens, Washington*, *U.S. Geol. Surv. Prof. Pap*., *1250*, 193–200, 1981.

Casadevall, T. J., W. I. Rose, T. Gerlach, L. P. Greenland, J. Ewert, R. Wunderman, and R. Symonds, Gas emissions and the eruptions of Mount St. Helens through 1982, *Science*, *221*, 1383–1385, 1983.

Casadevall, T. J., J. B. Stokes, L. P. Greenwood, L. L. Malinconico, J. R. Casadevall, and B. T. Furukawa, SO_2 and CO_2 emission rates at Kilauea Volcano, 1979–1984, in *Volcanism in Hawaii*, edited by R. Decker, T. Wright, and P. Stauffer, *U.S. Geol. Surv. Prof. Pap*., *1350*, 771–780, 1987.

Chartier, T. A., W. I. Rose, and J. B. Stokes, Detailed record of SO_2 emissions from Puu Oo between episodes 33 and 34 of the 1983–1986 ERZ eruption, Kilauea, Hawaii, *Bull. Volcanol*., *50*, 215–228, 1988.

Clough, S. A., F. X. Kneizys, and R. W. Davies, Line shape and the water vapor continuum, *Atmos. Res*., *23*, 229–241, 1989.

Crisp, J. A., A. B. Kahle, and E. A. Abbott, Thermal infrared spectral character of Hawaiian basaltic glasses, *J. Geophys. Res*., *95*, 21,657–21,669, 1990.

Daag, A. S., et al., Monitoring sulfur dioxide emission at Mount Pinatubo, in *Fire and Mud: Eruptions and Lahars of Mount Pinatubo, Philippines*, edited by C. G. Newhall and R. S. Punongbayan, pp. 409–414, Univ. of Wash. Press, Seattle, 1996.

Elias, T., A. J. Sutton, and J. B. Stokes, Current SO_2 emissions at Kilauea Volcano: quantifying scattered degassing sources, *Eos Trans. AGU*, *74*(43), Fall Meet. Suppl., 670–671, 1993.

Ferrare, R. A., S. H. Melfi, D. N. Whiteman, K. D. Evans, F. J. Schmidlin, and D. O'C. Starr, A comparison of water vapor measurements made by Raman lidar and radiosondes, *J. Atmos. Oceanic Technol*., *12*, 1177–1195, 1995.

Francis, P. W., A. Maciejewski, C. Oppenheimer, C. Chaffin, and T. Caltabiano, SO_2:HCl ratios in the plumes from Mt. Etna and Vulcano determined by Fourier transform spectroscopy, *Geophys. Res. Lett*., *22*, 1717–1720, 1995.

Gillespie, A. R., A. B. Kahle, and R. E. Walker, Color enhancement of highly correlated images, I, Decorrelation and HSI contrast stretches, *Remote Sens. Environ*., *20*, 209–235, 1986.

Graf, H.-F., J. Feichter, and B. Langmann, Volcanic sulfur emissions: Estimates of source strength and its contribution to the global sulfate distribution, *J. Geophys. Res*., *102*, 10,727–10,738, 1997.

Kahle, A. B., A. R. Gillespie, E. A. Abbott, M. J. Abrams, R. E. Walker, G. Hoover, and J. P. Lockwood, Relative dating of Hawaiian lava flows using multispectral thermal images: A new tool for geologic mapping of young volcanic terranes, *J. Geophys. Res*., *93*, 15,239–15,251, 1988.

Kahle, A. B., F. D. Palluconi, S. J. Hook, V. J. Realmuto, and G. Bothwell, The Advanced Spaceborne Thermal Emission and Reflectance Radiometer (ASTER), *Int. J. Imaging Syst. Technol*., *3*, 144–156, 1991.

Kanamitsu, M., Description of the NMC global data assimilation and forecast system, *Weather Forecast*., *4*, 335–342, 1989.

Krueger, A. J., L. S. Walter, C. C. Schnetzler, and S. D. Doiron, TOMS measurement of the sulfur dioxide emitted during the 1985 Nevado del Ruiz eruptions, *J. Volcanol. Geotherm. Res*., *41*, 7–15, 1990.

Krueger, A. J., L. S. Walter, P. K. Bhartia, C. C. Schnetzler, N. A. Krotkov, I. Sprod, and G. J. S. Bluth, Volcanic sulfur dioxide measurements from the Total Ozone Mapping Spectrometer (TOMS) instruments, *J. Geophys. Res*., *100*, 14,057–14,076, 1995.

Kyle, P. R., K. Meeker, and D. Finnegan, Emission rates of sulfur dioxide, trace gases, and metals from Mount Erebus, Antarctic, *Geophys. Res. Lett*., *17*, 2125–2128, 1990.

Kyle, P. R., L. M. Sybeldon, W. C. McIntosh, K. Meeker, and R. Symonds, Sulfur dioxide emission rates from Mount Erebus, Antarctica, in *Volcanological and Environmental Studies of Mount Erebus, Antarctica*, *Antarct. Res. Ser*., vol. 66, edited by P. R. Kyle, pp. 69–82, AGU, Washington, D. C., 1994.

Love, S. P., F. Goff, D. Counce, C. Siebe, and H. Delgado, Passive infrared spectroscopy of the eruption plume at Popocatepetl volcano, Mexico, *Nature*, *396*, 563–567, 1998.

McGee, K. A., The structure, dynamics, and chemical composition of noneruptive plumes from Mount St. Helens, 1980–88, *J. Volcanol. Geotherm. Res*., *51*, 269–282, 1992.

McGee, K. A., and T. M. Gerlach, Airborne volcanic plume measurements using a FTIR spectrometer, Kilauea Volcano, Hawaii, *Geophys. Res. Lett*., *25*, 615–618, 1998.

McGee, K. A., and A. J. Sutton, Eruptive activity at Mount St. Helens, Washington, USA, 1984–1988: A gas geochemistry perspective, *Bull. Volcanol*., *56*, 433–446, 1994.

Millan, M. M., Remote sensing of air pollutants: a study of some atmospheric scattering effects, *Atmos. Environ*., *14*, 1241–1253, 1980.

Moffat, A. J., and M. M. Millán, The applications of optical correlation techniques to the remote sensing of SO_2 plumes using sky light, *Atmos. Environ*., *5*, 677–690, 1971.

Mori, T., K. Notsu, Y. Tohjima, and H. Wakita, Remote detection of HCl and SO_2 in volcanic gas from Unzen Volcano, Japan, *Geophys. Res. Lett*., *20*, 1355–1358, 1993.

Naughton, J. J., J. V. Derby, and R. B. Glover, Infrared measurements on volcanic gas and fume: Kilauea eruption, 1968, *J. Geophys. Res*., *74*, 3273–3277, 1969.

Realmuto, V. J., The potential use of Earth Observing System data to monitor the passive emission of sulfur dioxide from volcanoes, in *Remote Sensing of Active Volcanism*, *Geophys. Monogr. Ser*., vol. 116, edited by P. J. Mouginis-Mark, J. A. Crisp, and J. H. Fink, pp. 101–115, AGU, Washington, D. C., 2000.

Realmuto, V. J., K. Hon, A. B. Kahle, E. A. Abbott, and D. C. Pieri, Multispectral thermal infrared mapping of the 1 October 1988 Kupaianaha flow field, Kilauea Volcano, Hawaii, *Bull. Volcanol*., *55*, 33–44, 1992.

Realmuto, V. J., M. J. Abrams, M. F. Buongiornio, and D. C. Pieri, The use of multispectral thermal infrared image data to estimate the sulfur dioxide flux from volcanoes: A case study from Mount Etna, Sicily, July 29, 1986, *J. Geophys. Res*., *99*, 481–488, 1994.

Realmuto, V. J., A. J. Sutton, and T. Elias, Multispectral thermal

infrared mapping of sulfur dioxide plumes: A case study from the East Rift Zone of Kilauea Volcano, Hawaii, *J. Geophys. Res*., *102*, 15,057–15,072, 1997.

Rose, W. I., R. L. Chuan, W. F. Giggenbach, P. R. Kyle, and R. B. Symonds, Rates of sulfur dioxide and particle emissions from White Island volcano, New Zealand, and an estimate of the total flux of major gaseous species, *Bull. Volcanol*., *48*, 181–188, 1986.

Rose, W. I., G. Heiken, K. Wohletz, D. Eppler, S. Barr, T. Miller, R. L. Chuan, and R. B. Symonds, Direct rate measurements of eruption plumes at Augustine volcano: A problem of scaling and uncontrolled variables, *J. Geophys. Res*., *93*, 4485–4499, 1988.

Rothman, L. S., et al., The HITRAN database: 1986 edition. *Applied Optics*, *26*, 4058–4097, 1987.

Rothman, L. S., et al., The HITRAN molecular spectroscopic database and HAWKS (HITRAN Atmospheric Workstation): 1996 edition, *J. Quant. Spectrosc. Radiat. Transfer*, *60*, 665–710, 1998.

Salisbury, J. W., and D. M. D'Aria, Emissivity of terrestrial materials in the 8–14 μm atmospheric window, *Remote Sens. Environ*., *42*, 83–106, 1992.

Schubert, S. D., R. B. Rood, and J. Pfaendtner, An assimilated dataset for earth-science applications, *Bull. Am. Meteorol. Soc*., *74*, 2331–2342, 1993.

Sparks, L., Accelerated line-by-line calculation of spectral absorption coefficients with high numerical accuracy, in *Optical Remote Sensing of the Atmosphere*, *Tech. Dig. Ser*., vol. 2, pp. 68–70, Opt. Soc. of Am., Washington, D. C., 1995.

Sparks, L., Efficient line-by-line calculation of absorption coefficients to high numerical accuracy, *J. Quant. Spectrosc. Radiat. Transfer*, *57*, 631–650, 1997.

Stoiber, R. E., L. L. Malinconico, and S. N. Williams, Use of the correlation spectrometer at volcanoes, in *Forecasting Volcanic Events*, edited by H. Tazieff and J. C. Sabroux, pp. 425–444, Elsevier Sci., New York, 1983.

Stoiber, R. E., S. N. Williams, and B. Huebert, Annual contribution of sulfur dioxide to the atmosphere by volcanoes, *J. Volcanol. Geotherm. Res*., *33*, 1–8, 1987.

Teggi, S., M. P. Bogliolo, M. F. Buongiorno, S. Pugnaghi, and A. Sterni, Evaluation of SO_2 emissions from Mt. Etna using diurnal and nocturnal multispectral IR and visible imaging spectrometer thermal infrared remote sensing images and radiative transfer models, *J. Geophys. Res*., *104*, 20,069–20,079, 1999.

Toth, R. A., Water vapor measurements between 590 and 2582 cm^{-1}: Line positions and strengths, *J. Mol. Spectrosc*., *190*, 379–396, 1998.

Toth, R. A., L. R. Brown, and C. Plymate, Self broadened widths and frequency shifts of water vapor lines between 590 and 2400 cm^{-1}, *J. Quant. Spectrosc. Radiat. Transfer*, *59*, 529–562, 1998.

Wade, C. G., An evaluation of problems affecting the measurement of low relative humidity on the United States radiosonde, *J. Atmos. Oceanic Technol*., *11*, 687–700, 1994.

Williams, S. N., N. C. Sturchio, M. L. Calvache, R. Mendez, A. Londoño, and N. García, Sulfur dioxide from Nevado del Ruiz volcano, Colombia: Total flux and isotopic constraints on its origin, *J. Volcanol. Geotherm. Res*., *42*, 53–68, 1990.

Worden, H. M., R. Beer, and C. P. Rinsland, Airborne infrared spectroscopy of 1994 western wildfires, *J. Geophys. Res*., *102*, 1287–1299, 1997.

Yamaguchi, Y., A. B. Kahle, H. Tsu, T. Kawakami, and M. Pniel, Overview of advanced spaceborne thermal emission and reflection radiometer (ASTER), *IEEE Trans. Geosci. Remote Sens*., *36*, 1062–1071, 1998.

Zapata, J. A., et al., SO_2 fluxes from Galeras Volcano, Colombia, 1989–1995: Progressive degassing and conduit obstruction of a Decade Volcano, *J. Volcanol. Geotherm. Res*., *77*, 195–208, 1997.

Zreda-Gostynska, G., and P. R. Kyle, Chlorine, fluorine, and sulfur emissions from Mount Etna, Antarctica, and estimated contributions to the antarctic atmosphere, *Geophys. Res. Lett*., *20*, 1959–1962, 1993.

V. J. Realmuto, Jet Propulsion Laboratory, Visualization and Earth Science Applications Group, MS 168-514, 4800 Oak Grove Drive, Pasadena, CA 91109. (vince.realmuto@jpl.nasa.gov)

H. M. Worden, Jet Propulsion Laboratory, MS 183-301, 4800 Oak Grove Drive, Pasadena, CA 91109. (helen.worden@jpl.nasa.gov)

(Received October 8, 1999; revised May 4, 2000;
accepted May 10, 2000.)